Helmholtz bright soliton splitting at nonlocal nonlinear interfaces

Zhiwei Shi
School of Information Engineering, Guangdong University of Technology, Guangzhou 510006, People's Republic of China

Qi Guo*
Laboratory of Nanophotonic Functional Materials and Devices, South China Normal University, Guangzhou 510631, People's Republic of China

Huagang Li†
Department of Physics, Guangdong University of Education, Guangzhou 510303, People's Republic of China
(Received 17 October 2013; published 30 December 2013)

We study Helmholtz bright soliton splitting at nonlocal nonlinear interfaces. Based on the framework of the Helmholtz theory, we demonstrate that bright soliton breakup depends on angle of incidence, nonlinear refractive index mismatch at the interface, and degree of nonlocality. Interestingly, the change of the degree of nonlocality can introduce collision and oscillation of solitons.

DOI: 10.1103/PhysRevA.88.063848 PACS number(s): 42.65.Tg, 42.25.Gy

I. INTRODUCTION

In the seminal works, people numerically observed that the planar boundary separating two dielectric media, where at least one of them is nonlinear (Kerr-type), can produce the breakup of an incident Gaussian soliton beam into multiple output solitons [1]. Wright and co-workers demonstrated numerically that external excitation of a nonlinear waveguide can produce sequential threshold behavior via multisoliton emission from the waveguide. This behavior is similar to that predicted to occur at a nonlinear interface [2]. In 2004, Aleshkevich and co-workers reported the results of numerical studies of the fission of N-soliton bound states at the interface formed by a Kerr nonlinear medium and a linear dielectric in a planar waveguide [3]. In this scenario, the number of solitons resulting from the reflection of multisoliton bound states has been reported to possess a strong angular character [3]. Subsequently, people addressed the reflection of vector solitons, comprising several components that exhibit multiple field oscillations, at the interface between two nonlinear media. They revealed that reflection causes fission of the input signal into sets of solitons propagating at different angles [4].

With the paraxial approximation, one has studied the physics of solitons impinging on planar boundaries separating two Kerr-type media using the nonlinear Schrödinger (NLS) equation. The particlelike approach [5] has succeeded in accounting for incident optical beam breakup into multiple self-focused channels and to deal with multiple reflection and transmission at multiple interfaces. Each new component generated can be treated as a separate equivalent particle moving in its own equivalent potential [6]. Nevertheless, most nonlinear phenomena arising at nonlinear interfaces have an angular component which is largely removed in any NLS-based analysis due to the assumed paraxial approximation [7]. This limitation is overcome using a Helmholtz nonparaxial framework. Nonparaxiality can refer to two different contexts of distinct nonparaxial character: high intensity and large angles of propagation [8–10]. The first type of nonparaxiality results from the evolution of ultranarrow beams in nonlinear media. In 1993, Akhmediev *et al*. cast doubt on the suitability and limitations of the normalized NLS equation for describing the evolution of such beams [9]. The scalar theory of the self-focusing of an optical beam is not valid for a very narrow beam, and a vector nonparaxial theory is developed from the vector Maxwell equations [10,11]. Based on these equations, Crosignani *et al*. have reported and analyzed bright [12] and dark [13] nonparaxial solitons. In contrast to the first type, the second type of nonparaxiality arises from the rapid evolution of the field envelope of a broad (when compared to the wavelength) beam propagating at a large angle to the longitudinal axis [8]. The scalar nonlinear Helmholtz (NLH) equation well describe this nonparaxiality and overcome the limitations of the NLS [14,15]. Exact analytical soliton solutions have been found in a focusing Kerr-type medium [14]. Nonparaxial theory based on NLH equation has also been applied to find dark Kerr [15], two-component [16], boundary [17], and bistable [18] Helmholtz soliton solutions. At nonlinear interfaces, soliton refraction effects have a strong inherent angular character and constitute an excellent test bed for nonparaxial Helmholtz theory [8,19–21]. Especially, soliton breakup occurring at the planar boundary separating two Kerr focusing and defocusing media was analyzed within the framework of the Helmholtz theory where the full angular content of the problem was preserved [21].

However, thus far soliton splitting at nonlocal nonlinear interfaces with the second type of nonparaxiality has not been studied. A nonlocal nonlinear response played an important role on the optical spatial solitons over the years. Nonlocality exists in different physical settings, as nematic liquid crystals [22], photorefractive media [23], thermal [24,25], and so on. Various degree of nonlocality given by the width of the nonlocal response function and the intensity profile of the beam can be divided into four types, like local, weakly nonlocal, general nonlocal, and highly nonlocal response [26,27]. In this paper, we numerically investigate the soliton splitting at nonlinear interfaces with the second type of

*guoq@scnu.edu.cn
†lihuagang@gdei.edu.cn

nonparaxiality in the nonlocal nonlinear medium. We find that the breakup number of solitons, the refraction power, and angle of refraction in the nonlocal nonlinear medium can be affected by angle of incidence, nonlinear refractive index mismatch at the interface, and degree of nonlocality. We devote Sec. II to a detailed description of the theory model of Helmholtz bright soliton splitting at the nonlocal nonlinear interfaces. Section III is devoted to studying the influence of angle of incidence, nonlinear refractive index mismatch at the interface, and degree of nonlocality on soliton breakup. Section IV summarizes the main conclusions of the paper.

II. THEORY MODEL

The scheme used in the Helmholtz analysis of nonlocal nonlinear interfaces is illustrated in Fig. 1. The dashed line represents the planar boundary separating two different nonlinear media. Medium 1 is a local nonlinear medium, and medium 2 is a nonlocal nonlinear medium. θ_{in} denotes an angle (in unscaled coordinates) of the interface and the transversal reference direction x, that is, the angle of incidence. Here we define angles of incidence and refraction as those made with the normal to the interface.

For the simple two-dimensional case, the time-independent complex optical field envelope $E(X,Z)$ of a continuous wave TE-polarized beam satisfies the Helmholtz equation [8],

$$\frac{\partial^2 \vec{E}}{\partial Z^2} + \frac{\partial^2 \vec{E}}{\partial X^2} + k_0^2 n^2(\vec{E})\vec{E} = 0. \tag{1}$$

Introducing a normalization appropriate to a forward-propagating beam, $E(X,Z) = A(X,Z)\exp(ik_1 Z)$ ($k_1 = n_{01}k_0$ is spatial wave number in medium 1), where $k_0 = \omega/c$ is the propagation constant in vacuum, c is the speed of light, ω is the frequency, and n_{01} is the linear refractive index of a first Kerr-type nonlinear material (medium 1) with total refractive index $n_{01} + \alpha_1|E|^2$, where α_1 is the nonlinear coefficient and $\alpha_1 \ll n_{01}$. For medium 2, a nonlocal nonlinearity $n(\vec{E}) = n_{02} + \Delta n$ and assuming that the approximation $n^2(\vec{E}) = n_{02}^2 + 2n_{02}\Delta n$. n_{02} is the linear refractive index; Δn is the nonlinear induced change of the refractive index, which satisfies

$$w_m^2 \frac{\partial^2 \Delta n}{\partial X^2} - \Delta n + \alpha_2|\vec{E}| = 0, \tag{2}$$

where α_2 is the nonlinear coefficient, and w_m is the characteristic length of the nonlinear response. Without further approximation, we have employed the following normalizations: $z = Z/L_D$, $x = \sqrt{2}X/w_0$, $u(x,z) = \sqrt{k_1\alpha_1 L_D/n_{01}}A(x,z)$, $\Delta n = \alpha_2 n_{01}\phi/(k_1\alpha_1 L_D)$. w_0 is a transverse scale parameter that we shall later relate to the width of nonparaxial soliton beams. This scale parameter can also be considered as equivalent to the waist of a (reference) paraxial Gaussian beam, at $z = 0$, which has a diffraction length $L_D = kw_0^2/2$. So, we get the following nonparaxial nonlinear Schrödinger equation (NNSE) for the dimensionless amplitude u of the light field coupled to the equation for normalized nonlinear induced change of the refractive index ϕ,

$$\kappa\frac{\partial^2 u}{\partial z^2} + i\frac{\partial u}{\partial z} + \frac{1}{2}\frac{\partial^2 u}{\partial x^2} + |u|^2 u = \left[\frac{\Delta}{4\kappa} + |u|^2 - \alpha\phi\right]\chi(x,z)u, \tag{3a}$$

$$d^2\frac{\partial^2 \phi}{\partial x^2} - \phi + |u|^2 = 0 \quad \text{(medium 2)}, \tag{3b}$$

where $\kappa = 1/(k^2 w_0^2)$ is the nonparaxial parameter of the NNSE [7,8,14–21] and $d = w_m/(\sqrt{2}w_0)$ stands for the degree of nonlocality of the nonlinear response. In the limits $\kappa \to 0$ and $d \to 0$, the nonlinear Schrödinger equation can be recovered from the system (3) which describes a local nonlinear response at $d \to 0$ and a strongly nonlocal response at $d \to \infty$. $\chi(x,z)$ accounts for the planar boundary which separates the two media, so it takes values 0 or 1 when (x,z) is in medium 1 or medium 2, respectively. In the particular case that the boundary is situated at $x = 0$, one obtains the Heaviside function $\chi(x,z) = H(x)$. $\Delta = 1 - n_{02}^2/n_{01}^2$ and $\alpha = (n_{02}\alpha_2)/(n_{01}/\alpha_1)$ account for the linear and nonlinear refractive index mismatch at the interface, respectively. For Eq. (3b), we can also write it into the form of convolution,

$$\phi = \int_{-\infty}^{+\infty} R(x - x')I(x')dx', \tag{4}$$

where $I = I(x,z) = |u(x,z)|^2$. The real, localized, and symmetric function $R(x)$ is the response function of the nonlocal medium, whose width determines the degree of nonlocality. For a singular response, $R(x) = \delta(x)$, the refractive index change becomes a local function of the light intensity, $\phi = I(x,z)$; i.e., the refractive index change at a given point is solely determined by the light intensity at that very point. With increasing width of $R(x)$ the light intensity in the vicinity of the point x also contributes to the index change at that point [27].

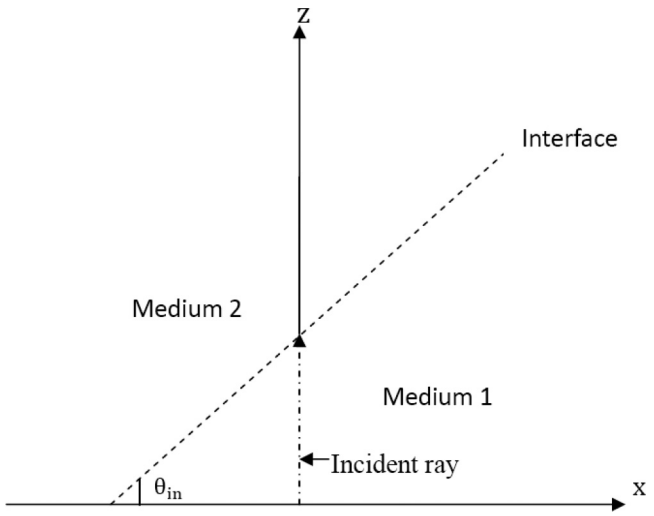

FIG. 1. Basic scheme used in this paper. All quantities are plotted in arbitrary dimensionless units.

III. SOLITON SPLITTING AT DIFFERENT INTERFACES

Our analysis of bright soliton splitting will be restricted to $\Delta = 0$; i.e., interfaces where linear refractive indices in both media are the same and the interfaces are nonlinear-step interfaces [8]. Under this condition, the amount of reflected power on such interfaces is reduced comparing with $\Delta \neq 0$ interfaces. Otherwise, these reflections could affect

the number of solitons appearing in the second medium. Second, we consider nonlinear-step interfaces with $\alpha > 1$, which is a sufficient condition for the existence of solitons in the second medium and establishes the necessary condition for the splitting of the solitons when crossing the interface [8]. Therefore, our work is almost restricted to mild on-axis nonparaxiality where any dramatic reduction in soliton width resulting from soliton breakup is avoided in order to maintain the validity of a scalar-based analysis of the problem [8]. In our study, we remove scenarios of very strong focusing.

To discuss the influence of the angle of incidence, nonlinear refractive index mismatch at the interface and degree of nonlocality on the Helmholtz bright solitons splitting at the interface, we use the split-step Fourier method (SSFM) and spectral renormalization method [28] to obtain the evolutions of solitons by solving the equations (3), where a solution guess for field distribution is $u(x) = \mathrm{sec\,h}(x)$. There is a need to explain that the red solid line and the green dot-dashed line denote the interface and the interface normal in all figures of the simulated evolutions of the beams in this paper, respectively. In our simulations, a fundamental bright soliton impinges on different nonlinear-step interfaces at same degree of nonlocality and angles of incidence, as illustrated in Fig. 2. Figure 2(a) shows the natural logarithm of the refraction power P and the effective angle of refraction θ_{eref} in medium 2 versus nonlinear refractive index mismatch at the interface α. We find that total power of the solitons in medium 2 will decrease with α. When α increases, the nonlinear-step increases; that is to say, the refractive index potential barrier at the interface increases. So, the power through the barrier decreases. The effective angle of refraction θ_{eref}, which is

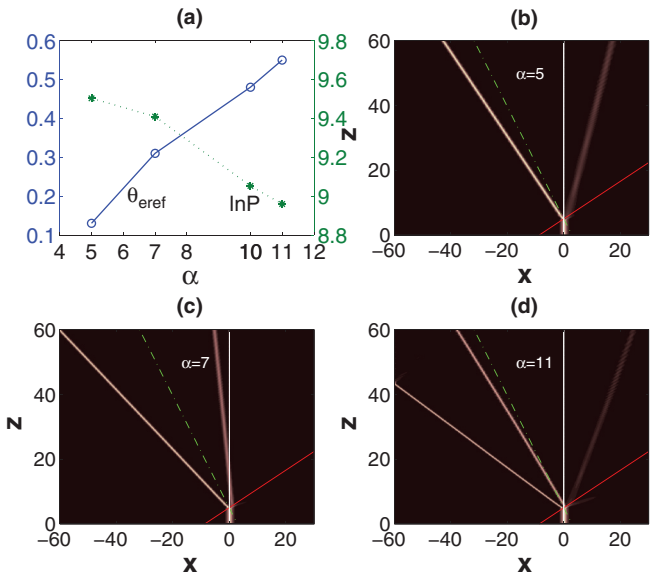

FIG. 2. (Color online) (a) The natural logarithm of the refraction power ln P (dotted green line) and the effective angle of refraction θ_{eref} (solid blue line) in medium 2 versus nonlinear refractive index mismatch at the interface α. Panels (b), (c), and (d) show the simulated evolutions of the beams at $\alpha = 5$, $\alpha = 7$, and $\alpha = 11$, respectively. The other parameter $\kappa = 1 \times 10^{-3}$, $\Delta = 0$, $\theta_{in} = 0.52$, and $d = 0.2$. The white solid lines denote $x = 0$, that is, the direction of the incidence. All quantities are plotted in arbitrary dimensionless units.

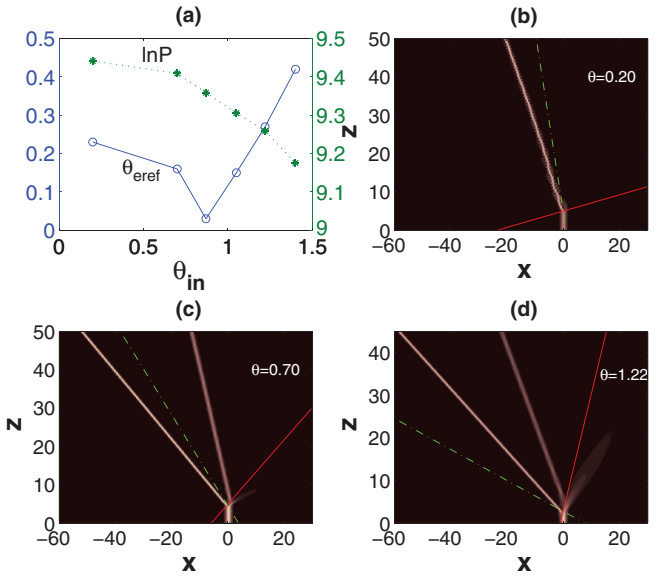

FIG. 3. (Color online) (a) The natural logarithm of the refraction power ln P (dotted green line) and the effective angle of refraction θ_{eref} (solid blue line) in medium 2 versus angle of incidence θ_{in}. Panels (b), (c), and (d) show the simulated evolutions of the beams at $\theta_{in} = 0.20, 0.70, 1.22$, respectively. The other parameter $\kappa = 1 \times 10^{-3}$, $\Delta = 0$, $\alpha = 7$, and $d = 0.2$. All quantities are plotted in arbitrary dimensionless units.

the angle of refraction of the largest-amplitude beam in medium 2, increases with α. The nonlinear refractive index mismatch at the interface may affect not only the number of solitons appearing in the second medium, but also the refraction scheme. Comparing Fig. 2(b) with Fig. 2(c), the smallest-amplitude beam is external refraction in Fig. 2(b); however, the beam is internal refraction in Fig. 2(c) [29]. Solitons impinging on an interface with $\alpha = 5, 7$ [see Figs. 2(b) and 2(c)] decompose into two solitonlike beams, while three are obtained with $\alpha = 11$ [see Fig. 2(d)].

Next, we discuss the influence of angle of incidence θ_{in} on the soliton splitting at the interfaces. Not only the number of solitons but also the amount of refracted power at the interface P or the angle of refraction of the largest amplitude beam θ_{eref} are so different. From Fig. 3(a), we can see that the angle of refraction of the largest amplitude beam θ_{eref} first decreases with angle of incidence θ_{in} and then increases with θ_{in}. When θ_{in} is smaller, the largest amplitude beam in medium 2 and the incident beam in medium 1 emerge on the same side of the interface normal, and θ_{eref} will decrease with θ_{in} . While θ_{in} exceeds a certain value, the largest amplitude beam in medium 2 and the incident beam in medium 1 appear on the opposite side of the interface normal, and θ_{eref} will increase with θ_{in}. The total power of the solitons P in medium 2 will decrease with θ_{in}. Solitons impinging on an interface with $\theta_{in} = 0.70, 1.22$ [see Figs. 3(c) and 3(d)] decompose into two solitonlike beams, while only one is obtained with $\theta_{in} = 0.20$ [see Fig. 3(b)].

At last, the influence of the degree of nonlocality d on the solitons splitting at the interfaces will be studied. A fundamental bright soliton impinges on the interfaces at different degree of nonlocality, as illustrated in Fig. 4. Figure 4 shows that the soliton splitting scheme actually depends on

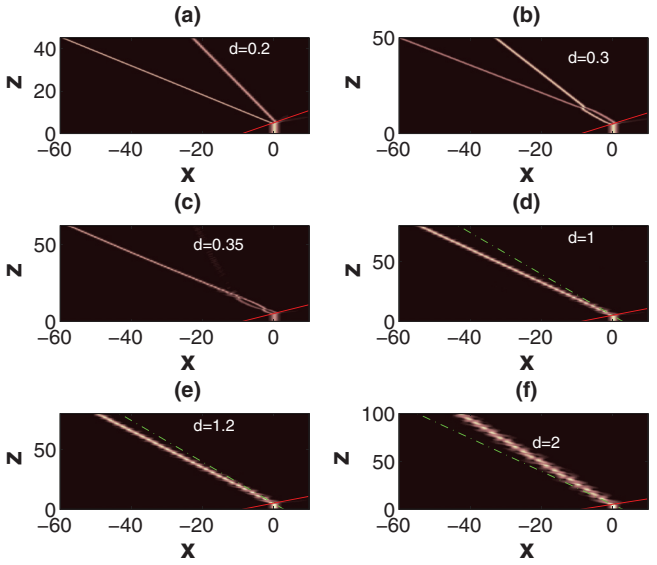

FIG. 4. (Color online) Panels (a)–(f) show the simulated evolutions of the beams for a range of d values varying from $d = 0.2$ to $d = 2$, respectively. The other parameter $\kappa = 1 \times 10^{-3}$, $\Delta = 0$, $\alpha = 10$, and $\theta_{in} = 0.52$. All quantities are plotted in arbitrary dimensionless units.

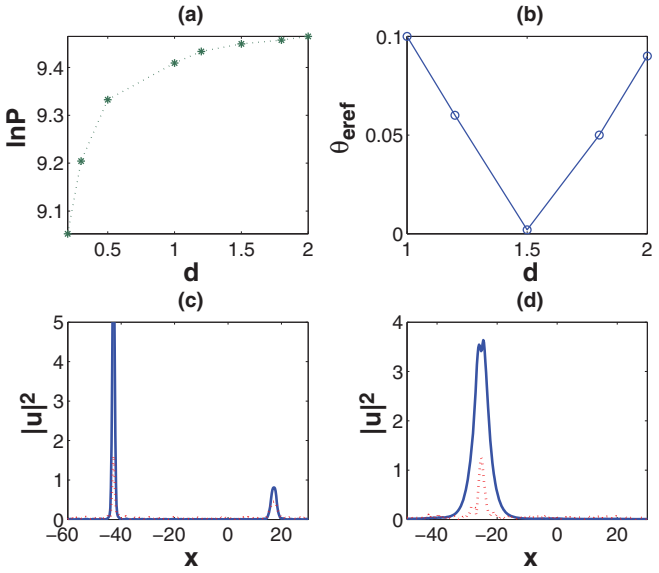

FIG. 5. (Color online) Panels (a) and (b) show the natural logarithm of the refraction power ln P (dotted green line) and the effective angle of refraction θ_{eref} (solid blue line) in medium 2 versus degree of nonlocality d, respectively. The other parameters are $\kappa = 1 \times 10^{-3}$, $\Delta = 0$, $\alpha = 10$, and $\theta_{in} = 0.52$. Panels (c) and (d) illustrate that the profiles of solitons $|u|^2$ (dotted red line) and the distribution of the refractive index $|\phi|$ (solid blue line) correspond to Fig. 2(b) and Fig. 4(f) at $z = 60$, respectively. All quantities are plotted in arbitrary dimensionless units.

the degree of nonlocality. At $d = 0.2$, solitons decompose into two solitonlike beams in medium 2, and the two beams interactions do not occur, as shown in Fig. 4(a). However, when the degree of nonlocality increases, the light intensity in the greater range of the point x contributes to the index change at that point [27], the two beams in medium 2 can collide shown in Figs. 4(b) and 4(c). Comparing Fig. 4(b) with Fig. 4(c), we can see that one collision occurs at $d = 0.3$, but two collisions occur at $d = 0.35$. In two figures, the two beams will separate after collision. However, it is clear that for a strong enough nonlocality the two spatial solitons trap each other. When the degree of nonlocality is greater, the smaller amplitude beam will periodically oscillate around the greater amplitude beam, and the oscillation amplitude increases with the degree of nonlocality. Interestingly, a similar phenomenon was noted in the intermediate process for dealing with incoherent solitons in "fast" nonlocal nonlinear media [30] and in the short-range interactions between strongly nonlocal spatial solitons [31]. These are shown in Figs. 4(d)–4(f). The amount of refracted power P will increase when d increases, as illustrated in Fig. 5(a). The angle of refraction of the greater amplitude beam θ_{eref} first decreases with d and then increases with d [see Fig. 5(b)]. When d is smaller, the largest amplitude beam in medium 2 and the incident beam in medium 1 emerge on the same side of the interface normal, and θ_{eref} will decrease with d . While d exceeds a certain value, the largest amplitude beam in medium 2 and the incident beam in medium 1 appear on the opposite side of the interface normal, and θ_{eref} will increase with d. There is a need to explain why we only show the cases of $d \geqslant 1$ in Fig. 5(b). We cannot explain angles of refraction in the cases of $d = 0.3, 0.35$, because the solitons collide.

A general feature that appears qualitatively striking about the data presented is the relative orientation of incident and refracted beams with respect to the interface normal. As shown in Figs. 3(d) and 4(f), the largest amplitude (refracted) beam in medium 2 and the incident beam in medium 1 emerging on the same side of the interface normal. However, Figs. 2(b)–2(d), Figs. 3(b) and 3(c), and Figs. 4(d) and 4(e) show that the largest amplitude beams emerging on the same side of the interface are normal to the incident beams. The reason for these situations is that medium 2 is a nonlocal nonlinear medium. A nonlocal nonlinear medium means that the response of the medium at a particular point is not determined solely by the wave intensity at that point (as in local media), but also depends on the wave intensity in its vicinity [27]. Further, the intensity dependence of the refractive index affects considerably the propagation of light waves in nonlinear media. As illustrated in Figs. 5(c) and 5(d), the largest amplitude beam must appear on the position of the largest refractive index. So, some plots here show refracted beams and the incident beams emerging on the same side of the interface normal.

IV. CONCLUSION

In conclusion, we have numerically analyzed soliton breakup at nonlinear interfaces separating two local and nonlocal nonlinear media. Based on the framework of the Helmholtz theory, we demonstrated that bright soliton breakup depends on angle of incidence, nonlinear refractive index mismatch at the interface and degree of nonlocality. The number of solitons, the refraction power, and angle of refraction in the nonlocal nonlinear medium can be affected by these parameters. Especially, the change of the degree of nonlocality can introduce collision and oscillation of solitons.

ACKNOWLEDGMENTS

This research is supported by the National Natural Science Foundation of China (Grant No. 11274125), the Postdoctoral Science Foundation of China (Grant No. 2013M531822), and the Natural Science Foundation of Guangdong Province of China (Grants No. S2012010009178 and No. S2012040007188).

[1] W. J. Tomlinson, J. P. Gordon, P. W. Smith, and A. E. Kaplan, Appl. Opt. **21**, 2041 (1982).
[2] E. M. Wright, G. I. Stegeman, C. T. Seaton, J. V. Moloney, and A. D. Boardman, Phys. Rev. A **34**, 4442 (1986).
[3] V. A. Aleshkevich, Y. V. Kartashov, A. S. Zelenina, V. A. Vysloukh, J. P. Torres, and L. Torner, Opt. Lett. **29**, 483 (2004).
[4] F. Ye, Y. V. Kartashov, and L. Torner, Opt. Lett. **32**, 394 (2007).
[5] A. B. Aceves, J. V. Moloney, and A. C. Newell, Phys. Rev. A **39**, 1809 (1989).
[6] A. B. Aceves, J. V. Moloney, and A. C. Newell, Phys. Rev. A **39**, 1828 (1989).
[7] J. Sánchez-Curto, P. Chamorro-Posada, and G. S. McDonald, Opt. Lett. **32**, 1126 (2007).
[8] J. Sánchez-Curto, P. Chamorro-Posada, and G. S. Mc-Donald, J. Opt. A **11**, 054015 (2009).
[9] N. Akhmediev, A. Ankiewicz, and J. M. Soto-Crespo, Opt. Lett. **18**, 411 (1993).
[10] S. Chi and Q. Guo, Opt. Lett. **20**, 1598 (1995).
[11] B. Crosignani, P. D. Porto, and A. Yariv, Opt. Lett. **22**, 778 (1997).
[12] B. Crosignani, A. Yariv, and S. Mookherjea, Opt. Lett. **29**, 1254 (2004).
[13] A. Ciattoni, B. Crosignani, S. Mookherjea, and A. Yariv, Opt. Lett. **30**, 516 (2005).
[14] P. Chamorro-Posada, G. S. McDonald, and G. New, J. Opt. Soc. Am. B **19**, 1216 (2002).
[15] P. Chamorro-Posada and G. S. McDonald, Opt. Lett. **28**, 825 (2003).
[16] J. M. Christian, G. S. McDonald, and P. Chamorro-Posada, Phys. Rev. E **74**, 066612 (2006).
[17] J. M. Christian, G. S. McDonald, and P. Chamorro-Posada, J. Phys. A **40**, 1545 (2007).
[18] J. M. Christian, G. S. McDonald, and P. Chamorro-Posada, Phys. Rev. A **76**, 033833 (2007).
[19] J. Sánchez-Curto, P. Chamorro-Posada, and G. S. McDonald, Opt. Lett. **35**, 1347 (2010).
[20] J. Sánchez-Curto, P. Chamorro-Posada, and G. S. McDonald, Opt. Lett. **36**, 3605 (2011).
[21] J. Sánchez-Curto, P. Chamorro-Posada, and G. S. McDonald, Phys. Rev. A **85**, 013836 (2012).
[22] C. Conti, M. Peccianti, and G. Assanto, Phys. Rev. Lett. **91**, 073901 (2003).
[23] M. Segev, B. Crosignani, A. Yariv, and B. Fischer, Phys. Rev. Lett. **68**, 923 (1992).
[24] C. Rotschild, O. Cohen, O. Manela, M. Segev, and T. Carmon, Phys. Rev. Lett. **95**, 213904 (2005).
[25] Y. V. Kartashov, V. A. Vysloukh, and L. Torner, Opt. Lett. **34**, 283 (2009).
[26] W. Królikowski, O. Bang, N. I. Nikolov, D. Neshev, J. Wyller, J. J. Rasmussen, and D. Edmundson, J. Opt. B **6**, S288 (2004).
[27] W. Królikowski and O. Bang, Phys. Rev. E **63**, 016610 (2000).
[28] M. J. Ablowitz and Z. H. Musslimani, Opt. Lett. **30**, 2140 (2005).
[29] J. M. Christian, E. A. McCoy, G. S. McDonald, J. Sánchez-Curto, and P. Chamorro-Posada, J. Phys. B: At. Mol. Opt. **2012**, 1 (2012).
[30] O. Cohen, H. Buljan, T. Schwartz, J. W. Fleischer, and M. Segev, Phys. Rev. E **73**, 015601(R) (2006).
[31] W. Hu, S. G. Ouyang, P. B. Yang, Q. Guo, and S. Lan, Phys. Rev. A **77**, 033842 (2008).